ACS Macro Letters

Letter

pubs.acs.org/macroletters

Template-Free Synthesis of Mesoporous Polymers for Highly Selective Enrichment of Glycopeptides

Tian Jin,[†,⊥] Zhichao Xiong,[†,∥,⊥] Xiang Zhu,*[,†,‡,⊥] Nada Mehio,[§] Yajing Chen,[†] Jun Hu,[†] Weibing Zhang,[†] Hanfa Zou,*[,∥] Honglai Liu,*[,†] and Sheng Dai*[,§]

[†]State Key Laboratory of Chemical Engineering and Department of Chemistry, East China University of Science and Technology, Shanghai, 200237, P. R. China

[‡]Department of Chemistry and Food Chemistry, Technische Universitat Dresden, Dresden 01062, Germany

[§]Chemical Sciences Division, Oak Ridge National Laboratory, Oak Ridge, Tennessee 37831, United States

[∥]Key Laboratory of Separation Sciences for Analytical Chemistry, Dalian Institute of Chemical Physics, The Chinese Academy of Sciences, Dalian, P. R. China

Supporting Information

ABSTRACT: A facile template-free strategy for the synthesis of mesoporous phenolic polymers with attractive porosities, nitrogen-containing functionalities, and intrinsic hydrophilic skeletons is presented. The resultant polymer has a high BET surface area (548 $m^2 g^{-1}$) and mesopore size (13 nm) and exhibits superior glycopeptide-capturing performance, thus, revealing the potential application of mesoporous polymers in highly selective glycopeptide enrichment. This general capture protocol may open up new opportunities for the development of glycoproteomes.

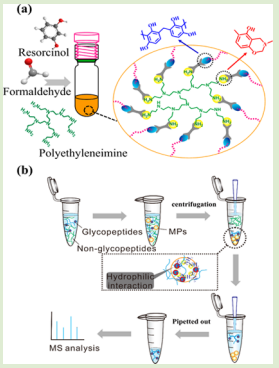

Protein N-glycosylation, the most predominant form of post-translational modifications, plays a vital role in many key cellular processes, for example, intracellular communication, molecular recognition, and immune response.[1,2] Alterations of the N-glycosylation sites and the attached glycans are frequently observed in diverse diseases. A large variety of glycoproteins have already been employed as disease biomarkers for disease diagnosis.[3] Nevertheless, owing to the inherent low abundance of glycopeptides in biological samples, the heterogeneity of glycosylation sites, and the high-content of interfering species, the analytical approach for the specific capture and identification of glycoproteins remains a challenge. Among the commonly employed glycopeptides-enrichment strategies, hydrophilic interaction liquid chromatography (HILIC)-based enrichment is particularly advantageous due to the high glycopeptide coverage, high compatibility with mass spectrometry, and excellent reproducibility. Though various HILIC-based materials have been prepared,[4−7] the drawbacks of these HILIC adsorbents like poor porosities and limited functional groups significantly restrain the enrichment efficiency toward glycopeptides. Mesoporous materials, due to their unique porosities and abundant binding sites inside the frameworks, have been successfully developed for peptides purification.[8−13] Typically, grafting a novel mesoporous silica with boronic acid groups leads to a high detection limit of glycopeptides.[14] However, it should be mentioned that the fabrication of such functionalized mesoporous materials entails using costly block copolymer-based templating agents and a multistep synthesis procedure, thus, potentially limiting the scale-up preparation. As such, the development of template-free and facile methods to prepare new mesoporous materials for efficiently trapping glycopeptides is particularly important.

Recently, porous polymers have emerged as a unique class of advanced porous materials because of their wide range of promising applications in energy, gas storage, and chemical separations.[15,16] In spite of their salient advantages of porosities and task-specific functionalities, which allow for the rapid and effective binding of biomolecules, so far they have never been introduced to separate glycoproteomes. It is believed that the use of porous polymers for the analysis of glycopeptides could not only expand the range of applications of porous polymers but also extend the library of porous materials developed for the specific enrichment of glycopeptides.

With these considerations in mind, herein, we propose a new template-free strategy for the fabrication of phenolic mesoporous polymers (MPs) for highly selective glycopeptide enrichment. The resultant MPs bear a number of attractive features, such as, high surface areas, large accessible porosities,

Received: April 7, 2015
Accepted: April 30, 2015
Published: May 1, 2015

DOI: 10.1021/acsmacrolett.5b00235
ACS Macro Lett. 2015, 4, 570−574

nitrogen-containing functionalities, and intrinsic hydrophilic skeletons, that facilitate highly specific and sensitive enrichment of glycopeptides from minute amounts of biological samples, thus, opening up new opportunities for the development of glycopeptides enrichment.

As shown in Scheme 1a, MPs can be facilely generated from a one-pot template-free polymerization between resorcinol, formaldehyde, and branched polyethylenimine (PEI). In a typical run, resorcinol was dissolved in a solvent mixture of ethanol and deionized water in a glass autoclave at 40 °C for 15 min (mins). Subsequently, variable quantities of PEI (50% in water) were added under constant stirring for another 20 min. Subsequently, formaldehyde aqueous solution was quickly injected and the mixture was stirred at the same temperature for 15 more mins. Then, the emulsion was heated at 120 °C for 12 h in an oven. Finally, the red-brown MPs (Figure S1 in the Supporting Information) were successfully obtained in good yields (Synthesis details can be found in the Experimental Section in the Supporting Information). The resulting MPs were found to be insoluble in common organic solvents (Figure S2 in the Supporting Information).

Scheme 1. (a) Synthesis Route to Mesoporous Polymer (MPs) and (b) Workflow of Rapid and Efficient Approach of Selective Glycopeptide Enrichment Protocol

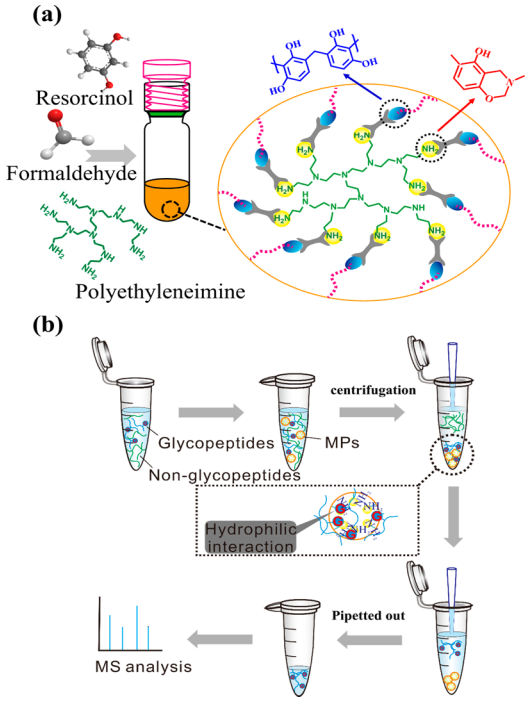

In order to confirm the successful formation of mesopores, the porosities of MPs were evaluated by nitrogen adsorption isotherms measured at 77 K. As shown in Figure 1a, type-IV isotherms with hysteresis loops characteristic of well-constricted mesopores were observed for MPs obtained from four different-molecular-weight (Mw) PEIs added in identical quantities. As the Mw of the PEI increased, the calculated Brunauer–Emmett–Teller (BET) surface areas and total pore volumes for MPs were slightly enhanced. Interestingly, the use of the PEI with the highest Mw (PEI-70000) yielded the largest BET surface area and pore volume, which were as large as 613 $m^2\ g^{-1}$ and 0.53 $cm^3\ g^{-1}$, respectively (MP-70000-25, Table 1).

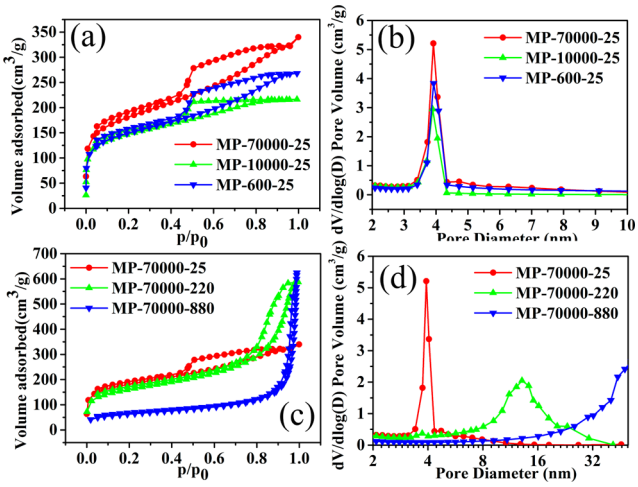

Figure 1. Nitrogen adsorption–desorption isotherms (a, c) and corresponding BJH pore size distributions (b, d) of MPs (25 means 25 mg PEI is added).

The pore size distribution (PSD) analysis of MPs based on the Barrett–Joyner–Halenda (BJH) model further confirmed a primary mesopore width of 3.9 nm and narrow width distributions (Figure 1b). In addition, similar mesoporous porosity was also observed for the polymer derived from the polymerization in the absence of PEI (Figure S3 in the Supporting Information). Therefore, the choice of the solvothermal condition for polymerization is a key component to the successful construction of good mesopores inside MPs. It is worth mentioning that the solvothermal route has been considered as a promising methodology for fabricating mesoporous polydivinylbenzene based materials.[17,18]

Besides the solvothermal effect, we also investigated the effect of PEI quantity on porosity. Because of the fact that the highest BET surface area was obtained for MP-70000-25, branched PEI-70000 was selected and used as the building block. As shown in Figure 1c, three different members of the MP-70000 series all exhibit accessible mesoporosities, as confirmed by N_2 adsorption–desorption isotherms. After increasing the amount of PEI-70000, the mesopores were greatly enlarged according to the PSD analysis (Figure 1d). A mesopore diameter as large as 13 nm can be achieved in the case of MP-70000-220, which also holds a promising BET surface area (S_{BET} = 548 $m^2\ g^{-1}$, Table 1). Moreover, adding a larger quantity of PEI-70000, 4 times larger than the quantity used to fabricate MP-70000-220, facilitated the formation of macropore inside the network and decreased the BET surface area (MP-70000-880, S_{BET} = 216 $m^2\ g^{-1}$). These results may clearly indicate that the quantity of added PEI plays a key role in influencing the porosities and surface areas for the resulting MPs. During the polymerization, the strong interaction between branched PEI and the primary polymerized species may result in further aggregation and give rise to interconnected mesoporous or macroporous particles. Consequently, the key to our successful synthesis of MPs through this novel template-free route lies in employing solvothermal conditions and branched PEI as a building block.

The structures of MPs were then characterized at the molecular level by solid state ^{13}C cross-polarization magic-angle spinning (CP/MAS) NMR (Figure S4 in the Supporting Information). Typically, in the spectrum of MP-70000-220, two peaks around ~51 and 29 ppm, which correspond to the

DOI: 10.1021/acsmacrolett.5b00235
ACS Macro Lett. 2015, 4, 570–574

Table 1. Textural Parameters of the Mesoporous Polymer (MPs)

sample	S_{BET} (m^2 g^{-1})	S_{micro} (m^2 g^{-1})	S_{meso} (m^2 g^{-1})	V_{total} (cm^3 g^{-1})	V_{micro} (cm^3 g^{-1})	N content (wt %)
MP-600-25	504	202	302	0.41	0.10	ND[a]
MP-10000-25	495	220	275	0.33	0.11	ND[a]
MP-70000-25	613	227	386	0.53	0.11	<0.3
MP-70000-220	548	162	386	0.87	0.08	0.56
MP-70000-880	216	46	170	0.97	0.02	2.70

[a]ND: not determined.

methylene groups in Ar−CH_2−N− and −$(CH_2)_2$−, were observed, respectively. These groups were products of a Mannich reaction that occurred during the polymerization process.[19,20] The formation of the benzoxazine ring (Ar−O−CH_2−N−) was confirmed by the signal at ∼80 ppm.[21] Moreover, the strong and broad peaks that occur between 100 and 175 ppm can be ascribed to the carbons in the aromatic rings of poly(resorcinol-formaldehyde) or poly(benzoxazine-PEI) networks.[19] The Fourier transform-infrared (FT-IR) spectrum of MP-70000-220 further confirms its chemical composition (Figure S5 in the Supporting Information). Absorption peaks at ∼1648 and 896 cm^{-1} can be assigned to the presence of in-plane and out-of-plane N−H deformation vibrations, respectively, suggesting the existence of amine segments.[22] Elemental analysis successfully revealed the presence of nitrogen within the networks (Table 1). As expected, greater quantities of added PEI afford greater degrees of nitrogen doping. MP-70000-880 bears a greater degree of nitrogen doping (2.70%, wt %) than MP-70000-220. Adequate thermal stabilities were obtained for MPs from their thermogravimetric analysis (TGA) analysis (Figure S6 in the Supporting Information). The morphologies were studied by field emission scanning analysis (Figure S7 in the Supporting Information). Amorphous characteristics of MPs were in good agreement with the results of their XRD results (Figure S8 in the Supporting Information). The transmission electron microscopy (TEM) images supported the existence of mesopores inside the network as well (Figure S9 in the Supporting Information). In addition, we further studied their water contact angles because of the surface effect on the enrichment of glycopeptides.[23] All three MP-70000s were hydrophilic with water contact angles lower than 40° (Figure S10 in the Supporting Information), suggesting promising hydrophilic interaction between the polymeric skeletons and glycopeptides.

As a proof of concept, we employed human IgG tryptic digest as a model biological sample in order to investigate the enrichment efficiency of MP-70000-220 which held the most attractive structural characters like high mesoporosity, BET surface area, nitrogen doping, and intrinsic hydrophilic matrix (Scheme 1b). As revealed by matrix-assisted laser desorption/ionization-time-of-flight mass spectrometry (MALDI-TOF MS) spectra analysis, an aqueous solution of human IgG at a concentration of 5 pmol μL^{-1}, which is difficult to detect among an abundance of nonglycopeptide peaks, shows signal-to-noise (S/N) ratio of GP10 of only 11 (Figure 2a). However, after enrichment with MP-70000-220 (Figure 2b), 20 glycopeptides (m/z 2200−3200) could be clearly detected with high MS intensity and S/N ratio (Table S1 in the Supporting Information). Because of the multivalent hydrophilic interactions between the hydroxyl groups on the glycans and the nitrogen-containing amine sites of MP-70000-220, the glycopeptides could be trapped on the internal and external

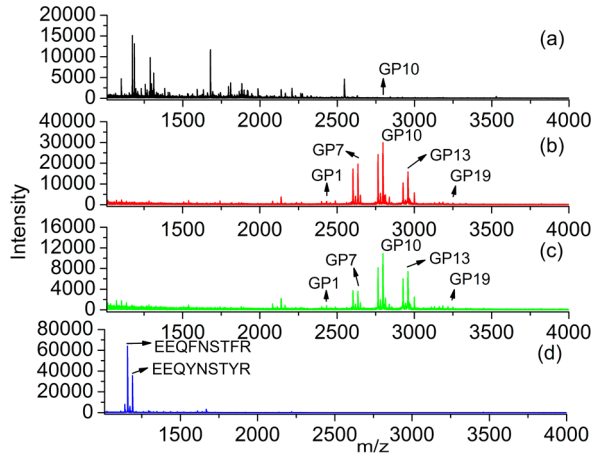

Figure 2. MALDI-TOF MS spectra of direct analysis of the 5 pmol of tryptic digest of human IgG (a), after enrichment by mesoporous polymer (MP-70000−220) (b), after enrichment by commercial HILIC beads (c), and then deglycosylated by PNGase F (d).

surface of MP-70000-220. Therefore, the S/N ratio of GP10 successfully increased to 678 with an enrichment factor (EF) of ∼62 (MS intensity ratio after and before the enrichment), indicating the excellent performance of MP-70000-220 in selectively enriching glycopeptides. To further demonstrate such a superior efficiency, a control experiment was conducted by using commercial HILIC beads as the adsorbents for the isolation of glycopeptide. As shown in Figure 2c and Table S3 in the Supporting Information, much lower EF of GP10 (25) was obtained. In addition, the eluted peptides can be deglycosylated by PNGase F. It should be mentioned that all the peaks of peptides (m/z > 2000) disappeared and only two deglycosylated peptides were detected (Figure 2d), which further ascertained that the peaks shown in Figure 2b all belonged to N-linked glycopeptides. The universality of the glycopeptide enrichment by MP-70000-220 was confirmed by taking chicken avidin as the sample. As conveyed in Figure S11 and Table S2 in the Supporting Information, 14 N-linked glycopeptides were enriched and detected by MP-70000-220. Furthermore, given the high surface area and accessible pores that facilitate mass transport, the enrichment process was accomplished in about 5 min. Clearly, these results indicate that MP-70000-220 has great potential for rapid and highly specific glycopeptide enrichment.

To get a better understanding of glycopeptide enrichment by MPs, two other MP-70000 series (MP-70000-25 and MP-70000-880) with different nitrogen doping underwent the enrichment processes as well. As shown in Figure S12 and Table S4 in the Supporting Information, these two MPs exhibit GP10 EFs of 36 and 8, respectively. The MS intensity and the S/N ratio of the captured glycopeptides were lower than the peaks displayed for MP-70000-220 (Figure 2b). Furthermore, it

DOI: 10.1021/acsmacrolett.5b00235
ACS Macro Lett. 2015, 4, 570−574

should be mentioned that MP-70000-220 exhibits higher MS intensity of the identified glycopeptides from the equal amount of human IgG tryptic digest than that observed for branched PEG brushes hybrid hydrophilic magnetic nanoparticles and multilayer polysaccharide coated magnetic nanoparticles.[24,25] The exceptional enrichment performance of MP-70000-220 may be due to a combination of high mesoporosities and nitrogen-containing functionalities inside the matrixes. In this regard, both should be taken into account simultaneously when designing new mesoporous materials for glycoproteomes.

Tryptic human IgG (3 μg) was used to evaluate the enrichment recovery of MP-70000-220 toward glycopeptides by the dimethyl labeling technique.[25] As shown in Table S5 in the Supporting Information, the recovery yield of seven selected glycopeptides was over 80.4%, thus, suggesting that MP-70000-220 is an ideal affinity material for the enrichment of glycopeptides. The reproducibility of the enrichment method was also tested using human IgG, and highly reproducible results were obtained (Figure S13 in the Supporting Information).

In addition, several human IgG tryptic digest with much lower concentrations of glycopeptides were treated with MP-70000-220 since the concentrations of glycopeptides are extremely low in complex, real biological samples. As shown in Figure S14 in the Supporting Information, for 5 fmol of human IgG tryptic digest, one target glycopeptide (GP8) was detected with a S/N ratio of 12, and the identified glycopeptides could be used as the fingerprint biomarker for the identification of human IgG. Thus, MP-70000-220 exhibits extreme sensitivity at the femtomole level and a detection limit that is lower than that of commercial HILIC beads (Figure S14d in the Supporting Information). The great enrichment performance toward trace amount of glycopeptide further suggests that MP-70000-220 can be used to discover and identify potential glycoprotein biomarkers.

A human serum sample (5 μL) was then employed as a real complex biological sample to evaluate the applicability of MP-70000-220. It is worth mentioning that the highly selective and sensitive enrichment methods are crucial in diagnostic and therapeutic biomarker discovery. However, the characterization of human serum glycoproteins remains a challenge because of the inherent low-content of glycoproteins and the existence of a high abundance of nonglycoproteins. After three independent analysis with nano LC−MS/MS, a total of 169 unique glycopeptides and 92 glycoproteins can be successfully identified (Table S6 in the Supporting Information), indicating MP-70000-220 exhibits better glycopeptide capture performance than commercial HILIC beads (Figure S15 in the Supporting Information).

In conclusion, mesoporous phenolic polymers bear a number of attractive features, such as large porosities, nitrogen doping, and intrinsic hydrophilic matrixes that are successfully fabricated through a facile template-free approach and can be used for highly selective enrichment of glycopeptides. MP-70000-220, which exhibited a high BET surface area (548 m^2 g^{-1}) and mesopore size (13 nm), efficiently sequestered glycopeptides, thus, highlighting the potential application of mesoporous polymers in highly selective glycopeptide enrichment processes. This general capture protocol may open up new opportunities for the development of glycoproteomes.

■ ASSOCIATED CONTENT

Supporting Information

Details of experimental procedures, Figures S1−S15, and Tables S1−S6. The Supporting Information is available free of charge on the ACS Publications website at DOI: 10.1021/acsmacrolett.5b00235.

■ AUTHOR INFORMATION

Corresponding Authors

*E-mail: xiang.zhu@tu-dresden.de.
*E-mail: hanfazou@dicp.ac.cn.
*E-mail: hlliu@ecust.edu.cn.
*E-mail: dais@ornl.gov.

Author Contributions

⊥T.J., Z.X., and X.Z. contributed equally.

Notes

The authors declare no competing financial interest.

■ ACKNOWLEDGMENTS

This work is supported by the National Basic Research Program of China (Grant 2013CB733501), the National Natural Science Foundation of China (Grants 91334203, 21376074, and 21321064), the 111 Project of Ministry of Education of China (Grant B08021), and the Fundamental Research Funds for the Central Universities. N.M. and S.D. were supported by the U.S. Department of Energy, Office of Science, Basic Energy Sciences, Chemical Sciences, Geosciences, and Biosciences Division.

■ REFERENCES

(1) Hart, G. W.; Copeland, R. J. *Cell* **2010**, *143*, 672−676.
(2) Service, R. F. *Science* **2012**, *338*, 321−323.
(3) Perego, P.; Gatti, L.; Beretta, G. L. *Nat. Rev. Cancer* **2010**, *10*, 523−523.
(4) Chen, C.-C.; Su, W.-C.; Huang, B.-Y.; Chen, Y.-J.; Tai, H.-C.; Obena, R. P. *Analyst* **2014**, *139*, 688−704.
(5) Selman, M. H. J.; Hemayatkar, M.; Deelder, A. M.; Wuhrer, M. *Anal. Chem.* **2011**, *83*, 2492−2499.
(6) Alley, W. R.; Mann, B. F.; Novotny, M. V. *Chem. Rev.* **2013**, *113*, 2668−2732.
(7) Kolarich, D.; Jensen, P. H.; Altmann, F.; Packer, N. H. *Nat. Protoc.* **2012**, *7*, 1285−1298.
(8) Liu, S.; Chen, H.; Lu, X.; Deng, C.; Zhang, X.; Yang, P. *Angew. Chem., Int. Ed.* **2010**, *122*, 7719−7723.
(9) Lu, Z.; Ye, M.; Li, N.; Zhong, W.; Yin, Y. *Angew. Chem., Int. Ed.* **2010**, *122*, 1906−1910.
(10) Tian, R.; Zhang, H.; Ye, M.; Jiang, X.; Hu, L.; Li, X.; Bao, X.; Zou, H. *Angew. Chem., Int. Ed.* **2007**, *119*, 980−983.
(11) Qin, H.; Gao, P.; Wang, F.; Zhao, L.; Zhu, J.; Wang, A.; Zhang, T.; Wu, R. a.; Zou, H. *Angew. Chem., Int. Ed.* **2011**, *50*, 12218−12221.
(12) Yan, J.; Li, X.; Yu, L.; Jin, Y.; Zhang, X.; Xue, X.; Ke, Y.; Liang, X. *Chem. Commun.* **2010**, *46*, 5488−5490.
(13) Zheng, J.; Xiao, Y.; Wang, L.; Lin, Z.; Yang, H.; Zhang, L.; Chen, G. *J. Chromatogr. A* **2014**, *1358*, 29−38.
(14) Xu, Y.; Wu, Z.; Zhang, L.; Lu, H.; Yang, P.; Webley, P. A.; Zhao, D. *Anal. Chem.* **2008**, *81*, 503−508.
(15) Wu, D.; Xu, F.; Sun, B.; Fu, R.; He, H.; Matyjaszewski, K. *Chem. Rev.* **2012**, *112*, 3959−4015.
(16) Liang, Y.; Fu, R.; Wu, D. *ACS Nano* **2013**, *7*, 1748−1754.
(17) Zhang, Y.; Wei, S.; Liu, F.; Du, Y.; Liu, S.; Ji, Y.; Yokoi, T.; Tatsumi, T.; Xiao, F.-S. *Nano Today* **2009**, *4*, 135−142.
(18) Liu, F.; Wang, L.; Sun, Q.; Zhu, L.; Meng, X.; Xiao, F.-S. *J. Am. Chem. Soc.* **2012**, *134*, 16948−16950.
(19) Gutiérrez, M. C.; Rubio, F.; del Monte, F. *Chem. Mater.* **2010**, *22*, 2711−2719.

DOI: 10.1021/acsmacrolett.5b00235
ACS Macro Lett. 2015, 4, 570−574

(20) Hao, G.-P.; Li, W.-C.; Qian, D.; Wang, G.-H.; Zhang, W.-P.; Zhang, T.; Wang, A.-Q.; Schüth, F.; Bongard, H.-J.; Lu, A.-H. *J. Am. Chem. Soc.* **2011**, *133*, 11378−11388.
(21) Ishida, H.; Ohba, S. *Polymer* **2005**, *46*, 5588−5595.
(22) Guo, D.-C.; Mi, J.; Hao, G.-P.; Dong, W.; Xiong, G.; Li, W.-C.; Lu, A.-H. *Energy Environ. Sci.* **2013**, *6*, 652−659.
(23) Zhang, Y.-W.; Li, Z.; Zhao, Q.; Zhou, Y.-L.; Liu, H.-W.; Zhang, X.-X. *Chem. Commun.* **2014**, *50*, 11504−11506.
(24) Xiong, Z.; Qin, H.; Wan, H.; Huang, G.; Zhang, Z.; Dong, J.; Zhang, L.; Zhang, W.; Zou, H. *Chem. Commun.* **2013**, *49*, 9284−9286.
(25) Xiong, Z.; Zhao, L.; Wang, F.; Zhu, J.; Qin, H.; Wu, R. a.; Zhang, W.; Zou, H. *Chem. Commun.* **2012**, *48*, 8138−8140.

DOI: 10.1021/acsmacrolett.5b00235
ACS Macro Lett. 2015, 4, 570−574